

Computer Simulation of the Forging of Fine Grain IN-718

R. Srinivasan, V. Ramnarayan¹, U. Deshpande, V. Jain², and I. Weiss

Mechanical and Materials Engineering Department
Wright State University, Dayton, Ohio 45435

¹ MTI, Inc. Johnstown, Pennsylvania 15904

² Mechanical and Aerospace Engineering Department
University of Dayton, Dayton, Ohio 45409

Abstract

In recent years there has been great emphasis on the use of computer-aided tools in process design. The key to the success of any computer modeling is the accurate knowledge of the mechanical and thermal properties of the various components of a manufacturing system. In order to develop a data base of forging properties of IN-718, isothermal constant strain rate compression tests were conducted on the annealed fine grain material over the temperature range 871°C to 1149°C (1600°F to 2100°F) and strain rate range 0.001 sec⁻¹ to 10 sec⁻¹. Constitutive equations developed from the results of these tests, along with experimentally measured heat transfer and friction coefficients were used in the program ALPID to simulate non-isothermal forging of double wedge specimens. The simulation results were compared with actual forging in an industrial forge press. The good agreement between simulation and forging results indicates that when an accurate and complete data base of materials properties is available, computer modeling can be used effectively to study forging.

This investigation was performed under the Edison Materials Technology Center (EMTEC) Core Technology Project No. CT-13. Support for the work is gratefully acknowledged. The authors would also like to thank Dr. Shesh Srivatsa of GE Aircraft Engines, for technical discussions during the course of this work.

Introduction

In recent years the field of metal forming has witnessed great emphasis on technologies associated with process modeling in manufacture. Traditional build and test methods for die design and selection of process variables have resulted in high tooling and setup costs, and in long lead times before production. The development of simulation programs, such as ALPID, MARC, and ADINA, has moved some of the trial-and-error involved in the conventional process design procedure from the shop floor to the computer, where many options can be investigated economically prior to an actual build-and-test. The key to the success of any simulation is accurate knowledge of the properties, both thermal and mechanical, of the major components of the metal forming system under the operating conditions of a manufacturing process. Handbooks of material properties report the properties of materials under service conditions. For an alloy such as IN-718, these include elastic moduli, thermal expansion coefficients, fatigue and creep data over a temperature range from room temperature to about 1200°F (650°C) and for small plastic strains. Forging of nickel base alloys is carried out at temperatures of about 1800°F (980°C) and to large plastic strains (> 100%) under non-isothermal conditions, and the handbook data is of little value for computer modeling under these processing conditions.

Forging Properties Data

A considerable effort has been undertaken to determine the flow behavior of workpiece materials, and a data base suitable for use in simulation programs is being developed. However, other necessary properties, such as thermal expansion coefficients, thermal conductivity, and elastic properties at elevated temperatures are not readily available, especially at temperatures encountered in the forging process. The availability of property data is even worse for die materials, for which almost no relevant data exist. Thermal and mechanical properties of die materials are needed in order to predict die stresses and distortions which affect the workpiece metal flow and final dimensions of the part. These properties are also needed to predict temperature distributions in both workpiece and dies. The current state of development of finite element analysis allows simulation models in which calculation of temperature and stress distributions are coupled. Thus, both thermal and mechanical properties are of critical importance in order to achieve accurate, realistic simulation models.

Material properties for forging simulations can be classified into the following groups:

Deformation behavior of workpiece and die materials:

During metal forming the workpiece material is subjected to large plastic deformation, while the die deformations are primarily elastic. The workpiece material constitutive model is a plastic flow law that describes the dependence of flow stress on strain, strain rate, and temperature. Many simple empirical constitutive equations have been formulated [2,3]. However, most engineering materials do not obey these relationships, especially when temperature variations are allowed. Since it is generally difficult to relate the gross deformation behavior to atomistic and crystalline deformation mechanisms, empirical constitutive relations have been developed for specific ranges of temperatures, strain rates, and strains.

Thermal properties of workpiece and die materials:

Thermal properties are necessary to predict temperature distributions in the workpiece and dies during forging. The important properties are heat capacity, thermal conductivity, coefficient of thermal expansion, and surface emissivity for radiative heat transfer. Since over 90% of the work of deformation is converted to heat, the thermal properties mentioned would determine the temperature distributions, and, therefore, the deformation behavior of the workpiece and dies.

Interface friction and heat transfer characteristics:

The interface between the workpiece and the dies determine the deformation behavior of the workpiece through two primary phenomena: the interface friction, and the interface heat transfer. Accurate mathematical description of both these features is difficult since they are affected by several factors, such as stress on the interface, temperature, and time. Simplifying assumptions are generally made. For example, the interface friction factor is assumed to be either a function of just the stress at the interface (Coulomb model) or a fraction of the flow stress of the workpiece material (constant shear factor model).[4] The latter model is frequently used in metal forming analysis.[5]

Experimental Determination of Forging Properties

The thermo-visco-plastic metal deformation simulation package ALPID [5] has gained wide acceptance in the forging industry as a computer based method for the analysis and the design of forging processes. In this study, the properties required to simulate forging using ALPID have been determined. Specifically, flow stress of the workpiece material as function of strain rate, temperature and strain, a single value of the constant shear stress friction factor, a single value for the heat transfer coefficient across the lubricated and insulated interface between the workpiece and the dies, and heat capacities of the workpiece and die materials.

Test Materials

The following materials were used in this investigation:

| | |
|---------------------|--|
| Workpiece material: | Fine grain IN-718 nickel base superalloy forging stock |
| Die material: | H-13 steel |
| Interface material: | Siltemp (silica cloth) + a proprietary lubricant of Wyman Gordon Co. |

The applicable properties described above were determined for each of the materials listed.

Flow Stress Measurements

Constitutive equations for metal deformation are of the following general form.[6]

$$\sigma = \sigma(\dot{\epsilon}, T, S),$$

where σ = flow stress
 $\dot{\epsilon}$ = strain rate
 T = temperature
 S = an evolutionary parameter representing prior thermomechanical history and accumulated deformation.

While $\dot{\epsilon}$ and T are state variables, S is not a true state variable. Constitutive equations for metal deformation, however, generally assume that for a given material, the starting condition, i.e., the thermomechanical history of the material, is fixed, and constitutive relations are developed assuming strain, ϵ , is a state variable.[6] Under these assumptions, isothermal constant true strain rate tests over the strain rate and temperature ranges of interest will yield the experimental data required to formulate the empirical relationships between stress, strain rate, temperature and strain.

Compression tests were conducted in the high temperature deformation test facility shown schematically in Figure 1. The facility consists of a 100 ton servohydraulic test frame with a controlled atmosphere radiant heat furnace. In order to obtain

constant strain rate, the displacement of the actuator is controlled by a signal from a microcomputer. The furnace control temperature was calibrated against the temperature measured by a thermocouple inserted into the middle of a dummy specimen. A linear relationship between the specimen temperature and the furnace set point temperature, with a regression coefficient > 0.9999 , assured an accuracy of the specimen temperature to $\pm 1^\circ\text{C}$ over the test temperature range. The strain rate and temperature ranges were as follows:

Strain Rate $\dot{\epsilon} = 0.001, 0.00316, 0.01, 0.0316, 0.1, 0.316, 1, 3.16, 10 \text{ sec}^{-1}$
 $\log(\dot{\epsilon}) = -3.0, -2.5, -2.0, -1.5, -1.0, -0.5, 0.0, 0.5, 1.0$
 Temperatures $1600^\circ, 1700^\circ, 1800^\circ, 1900^\circ, 2000^\circ, 2050^\circ, 2100^\circ, 2150^\circ \text{ F}$
 $871^\circ, 927^\circ, 982^\circ, 1038^\circ, 1093^\circ, 1121^\circ, 1149^\circ, 1177^\circ \text{ C}$

Cylindrical specimens 0.5 inch diameter and 0.75 inch height were machined by EDM from a 8 inch diameter slice of IN-718 forging stock. Approximately 100 tests were conducted over the 72 independent test conditions listed above. Tests were repeated to check reproducibility of data. All flow curves were corrected for deformation heating. [7]

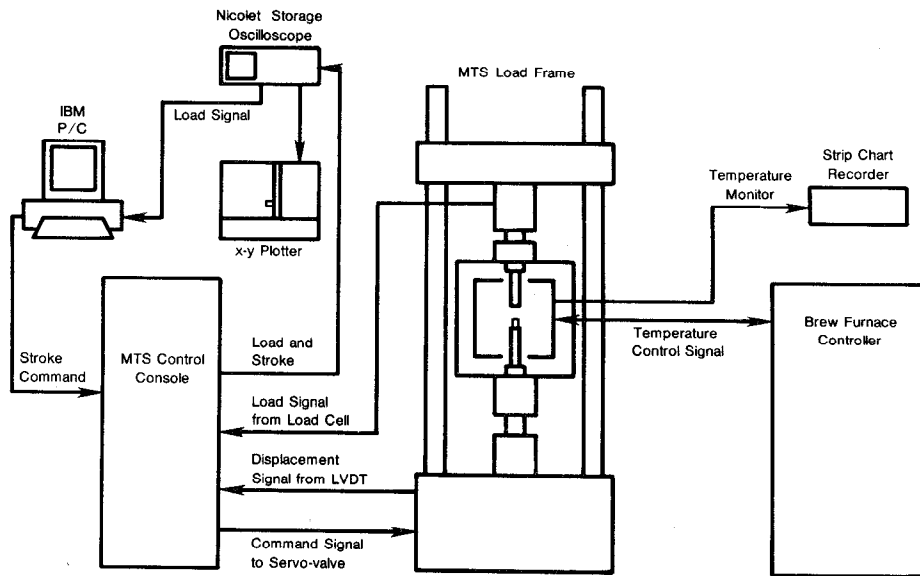


Figure 1. Schematic of the Deformation Testing Facility

Interface Friction and Heat Transfer Coefficient

Experimental methods to determine the interface friction and heat transfer coefficient provide information to considerable greater detail than is required by the computer program ALPID, which requires just single values for each of these parameters. The interface friction was determined by the ring test. [8,9] The interface heat transfer coefficient was measured using the method of Jain and Goetz. [10] The technique involves bringing a specimen heated to one temperature into contact with dies heated to a different temperature. Temperature gradients that develop are used to calculate the heat flux, and thereby the effective heat transfer coefficient across the interface, assuming steady state conduction equations apply. By choosing the specimen material, die material, and lubricant, it is possible to determine the interface heat transfer coefficient for a given process. [10]

Thermal Properties of the Workpiece and Die Materials

The thermal properties of the workpiece and die materials were determined at Purdue University's Thermophysical Properties Research Laboratory (TPRL).[11] The properties measured were the coefficient of thermal expansion, specific heat, and heat capacity over the temperature range of RT to 1200°C.

Physical Modeling Experiments

In order to validate computer simulation results, actual forging experiments were carried out on a 1500 ton industrial forge press at Wyman Gordon Co. Figure 2 shows the dimensions of the specimen used. The shape is axisymmetric, with a central cylindrical disk 0.625 in. thick and tapered sections above and below the cylinder. This shape has been variously called the double-wedge or the double-cone. Double wedge test specimens were machined out of IN-718 forging stock, wrapped in silica cloth (Siltemp) and heated to 1800°F. The specimens were then forged between H-13 dies at three initial target temperature of 1000°F, 1200°F and 1400°F, at nominal speeds of 7.5 in/min, 15.0 in/min, 22.5 in/min and 30 in/min.(Table 1) Load vs. time and stroke vs. time curves were recorded for each of the forging runs. In all cases, the final thickness of the forged pancakes was determined by the load capacity of the press, and was greater than the target thickness of 0.625 inch.

Computer Simulation Experiments

Figure 3 is a flow chart describing the scope of this work. Experimentally determined material properties, and forge press characteristics obtained from actual forging runs were used to simulate the forging of the double-wedge specimens. The stroke-time profile from the physical experiments were converted to velocity-time functions to describe the displacement of the dies.

The workpiece was discretized into 300 nodes and 266 four node quadrilateral elements. The dies were each discretized into 165 nodes and 140 four node quadrilateral elements. (Figure 4) For the rigid-viscoplastic analysis the nodes in the workpiece each had two degrees of freedom (translation in the x and y directions). For the thermal analysis the nodes in the workpiece and the dies had one degree of freedom (temperature). Table 2 lists the thermal parameters used in the simulations.

The constitutive equations to describe the deformation behavior of the workpiece material were developed from the compression test results, as described below.

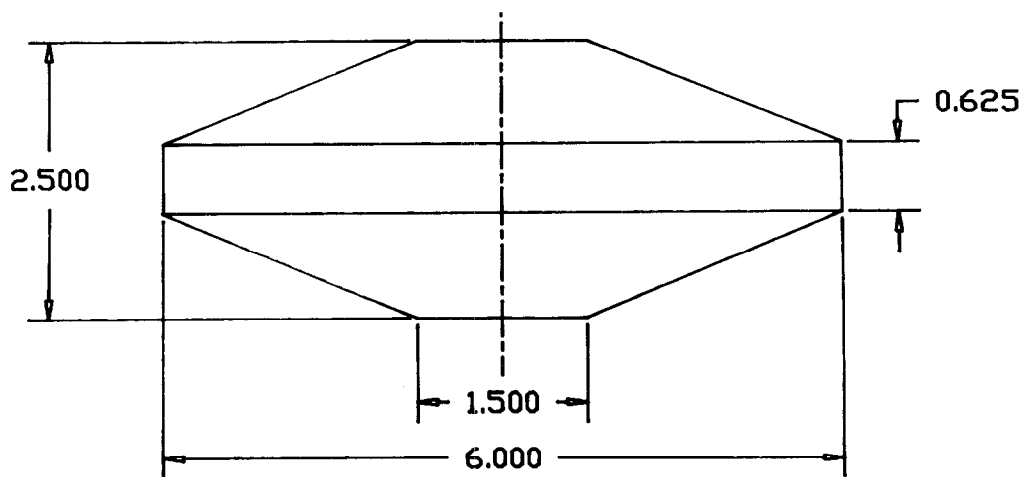


Figure 2. Dimensions of the Physical Modeling Specimens

Table 1. Forging Conditions

| Serial # | Die Temps. deg. F | Aim Cross-Head Speed in/min | Actual Cross-Head Speed in/min | Final Thickness (in) |
|----------|-------------------|-----------------------------|--------------------------------|----------------------|
| 6 | 1402-1410 | 7.5 | 7.2 | 0.80 |
| 8 | 1220-1224 | 7.5 | 7.3 | 0.83 |
| 14 | 996-1036 | 7.5 | 7.1 | 0.89 |
| 7 | 1192-1197 | 15.0 | 12.6 | 0.83 |
| 11 | 1001-1018 | 15.0 | 12.7 | 0.87 |
| 4 | 1391-1396 | 22.5 | 18.3 | 0.76 |
| 9 | 1230-1231 | 22.5 | 18.8 | 0.82 |
| 3 | 1411-1416 | 30.0 | 22.8 | 0.76 |
| 10 | 987-1224 | 30.0 | 22.8 | 0.82 |
| 13 | 987-1021 | 30.0 | 22.8 | 0.82 |

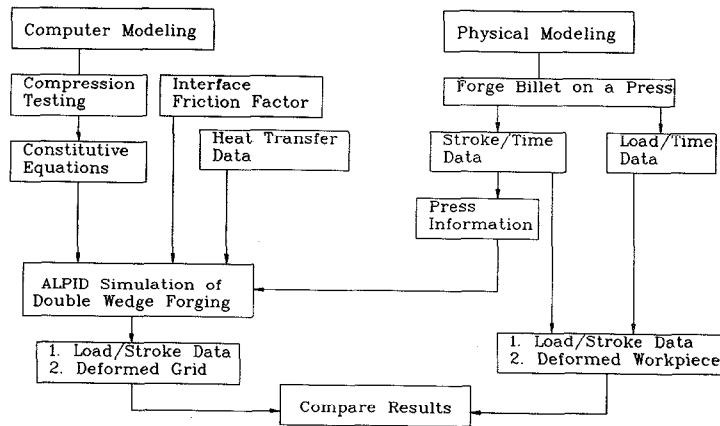


Figure 3. Scope of Investigation

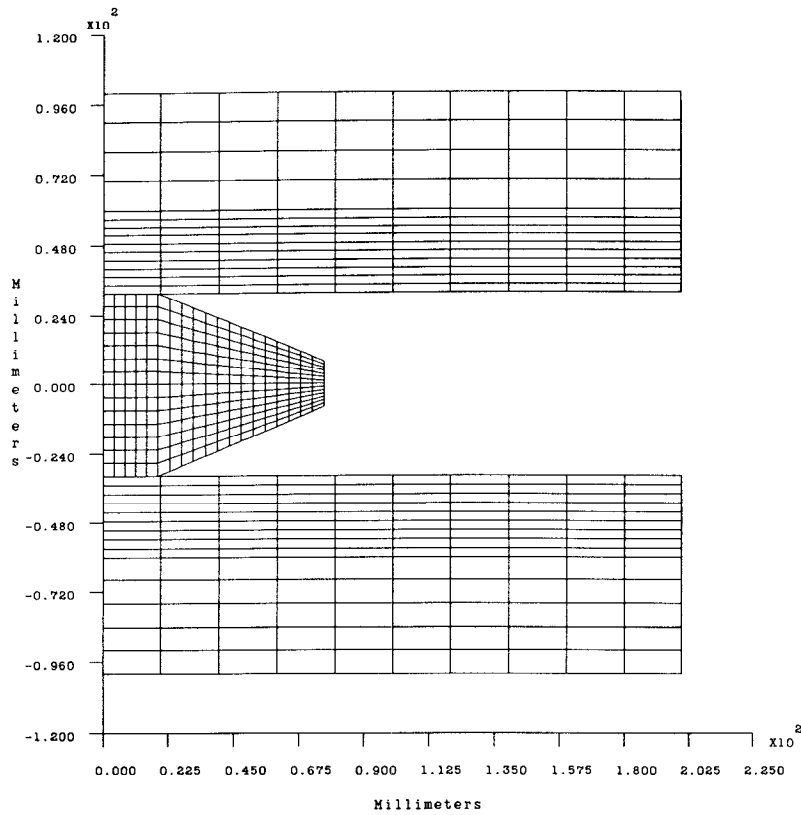


Figure 4. Finite Element Mesh used in Forging Simulations

Table 2. Thermal Parameters used in Forging Simulations

Thermal Properties

| | |
|--|---|
| Radiation Heat Transfer Coefficient | = 8.5×10^{-13} watt/m ² /K ⁴ |
| Convection Heat Transfer Coefficient | = 0.02 watt/m ² /°C |
| Interface Heat Transfer Coefficient | = 1.3114 watt/m ² /°C |
| Conduction Heat Transfer Coefficient | = 25 watt/m/°C |
| Specific Heat | = 600 J/kg/°C |
| Fraction of plastic work converted to heat | = 0.9 |
| Friction Coefficient | = 0.3 |

Constitutive Equations for IN-718

The results of the isothermal constant strain rate compression test were used to determine the deformation behavior of IN-718. Due to deformation heating, the flow stress tended to decrease with increasing strain. The effect was more significant at lower temperatures and higher strain rates where the stress level is higher and the time of deformation is shorter. The flow curves were corrected assuming all the flow softening is due to deformation heating. [7] Typical corrected flow curves are shown in Figures 5 and 6. The curves at all temperatures and strain rates show little dependence of stress on strain beyond a strain of approximately 0.3. Assuming flow stress is a function of only strain rate and temperature, at each temperature a

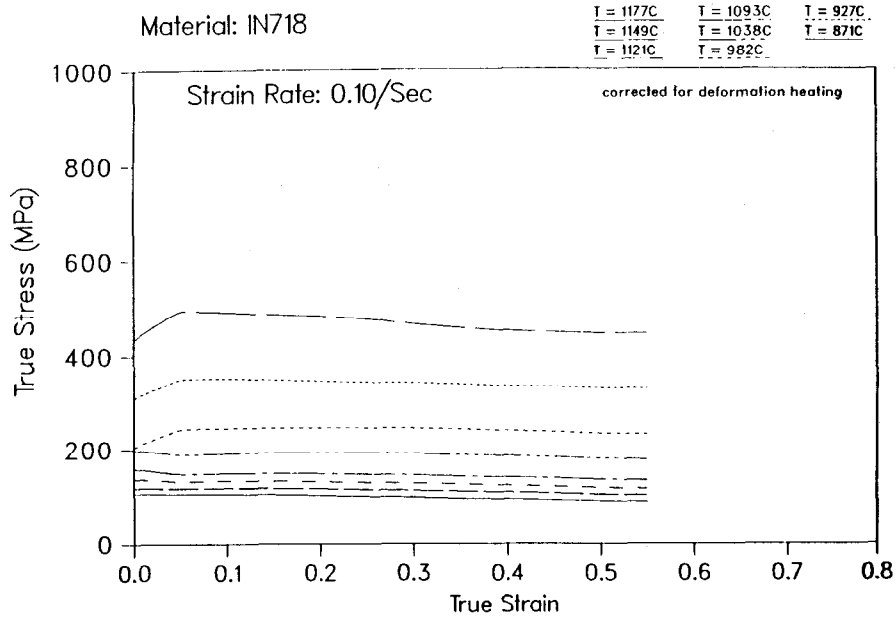


Figure 5. Flow Curves at Strain Rate = 0.01 s^{-1}

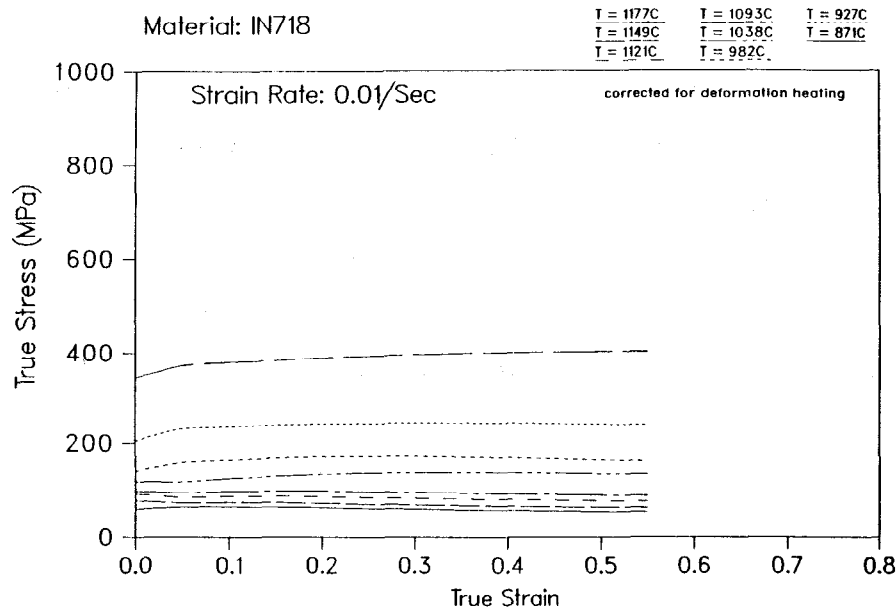


Figure 6. Flow Curves at Strain Rate = 0.1 s^{-1}

polynomial equation relating $\log(\sigma)$ and $\log(\dot{\epsilon})$ was determined. These equations were typically of the form:

$$\log(\sigma) = A + BX + CX^2 + DX^3$$

where $X = \log(\dot{\epsilon})$. Table 3 shows the constants in the above equations at different temperatures. Flow stresses at intermediate temperatures were obtained by linear interpolation of the constants.

Table 3. Coefficients of the Constitutive Equations

| Temperature C | Temperature F | A | B | C | D |
|------------------|------------------|-------|---------|-----------|-----------|
| 1177 | (2150) | 2.169 | 0.21269 | 0.020819 | 0.009133 |
| 1149 | (2100) | 2.238 | 0.17931 | -0.020659 | 0.002201 |
| 1121 | (2050) | 2.292 | 0.14630 | -0.052532 | -0.011510 |
| 1093 | (2000) | 2.343 | 0.13281 | -0.049116 | -0.009878 |
| 1038 | (1900) | 2.451 | 0.13567 | -0.010316 | 0.000951 |
| 982 | (1800) | 2.557 | 0.13084 | -0.009181 | 0.000911 |
| 927 | (1700) | 2.664 | 0.17746 | -0.008929 | 0.000000 |
| 871 | (1600) | 2.833 | 0.03349 | -0.101825 | -0.028949 |

Results and Discussions

The press characteristics for each forging run, in the form of displacement–time data, were used as a part of the input to the computer simulations. The simulations predicted several features of each forging run, such as, grid distortions, strain distributions in the workpiece, temperature distributions in the workpiece and dies, and load stroke curves. The overall shape of the deformed mesh and the load stroke curves were compared directly with experimental results. The trends in temperature and strain distributions were verified indirectly by studying the microstructure of the deformed specimens.

Load Stroke Curves

The duration of the forging runs varied from approximately 4.5 seconds to 15 seconds. Load and displacement recorded as a function of time by a strip chart recorder on the forge press were converted to load–stroke curves. Surprisingly, there was little variation among the ten different experiments. (Figure 7)

Figure 8 shows the comparison between the experimental and predicted load stroke curves for a typical forging run. Good agreement between experiment and predictions was obtained for all ten forging conditions.

Strain and Temperature Distributions

During the deformation of the double wedge specimen (Figure 2), the top and bottom

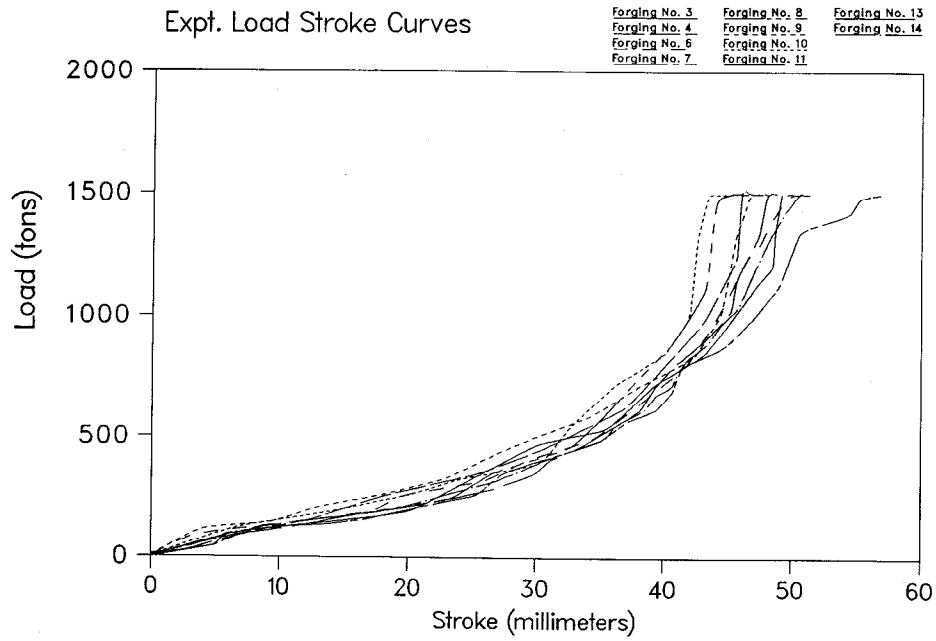


Figure 7. Load Stroke Curves of 10 Experimental Forging Runs

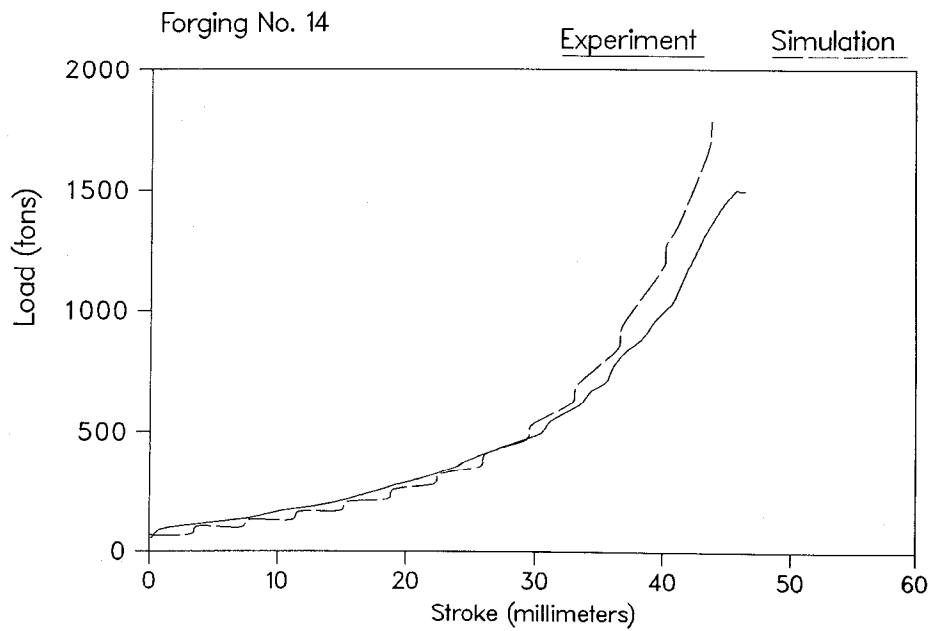


Figure 8. Comparison between Experimental and Simulation Load Stroke Curves

surfaces of the specimen in the hub region are in contact with the dies, and are subject to friction and heat loss to the die. As deformation progresses, the tapered surfaces contact the die, and are subject to the die contact effects of friction and chilling. The expected pattern of deformation under such scenario would be a lower strain in the regions close to the surface, and higher strain at the center of the specimen. The predicted strain distribution for Forging No. 3 was different from expectations (Figure 9). The strain distribution in the hub was typical of a simple upsetting, i.e., low strains in the die contact regions and higher towards the center. The strain contours in the initially tapered section of the specimen shows that the strains on the top and bottom surfaces are higher than in the middle of the disk.

Figure 10 shows the predicted temperature distributions in the forging. Though the initial die temperature (766°C, 1400°F) was over 200°C lower than the initial workpiece temperature (982°C, 1800°F), there is only a small little change in the workpiece temperature after forging, ranging from 959°C to 1107°C. Figure 11 shows the predicted strain distribution in an isothermally forged workpiece. The strain distribution in non-isothermal forging (Figure 9) and that in the isothermal forging (Figure 11) are similar. The simulations predict, therefore, that the deformation of the workpiece took place with almost no heat being lost to the dies. This can be attributed to the low value of the heat transfer coefficient at the die/workpiece interface. (Table 3) Since the deformation is occurring without a significant heat loss to the dies, and the starting workpiece temperature for all forgings was the same (982°C, 1800°F), there would be very little variation among the different forging runs and the load-stroke curves for all the runs were similar. (Figure 7)

FORGING NO 3

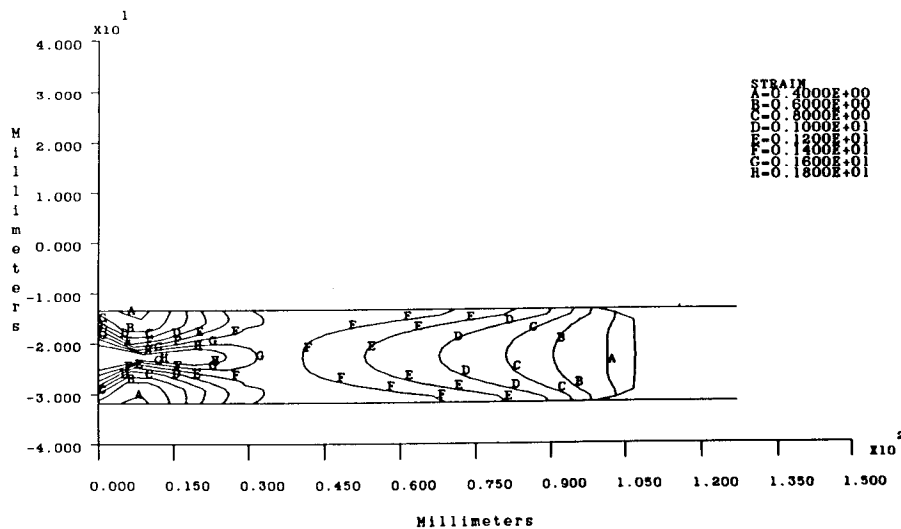


Figure 9. Predicted Strain Distribution in Forging No. 3

FORGING NO. 3

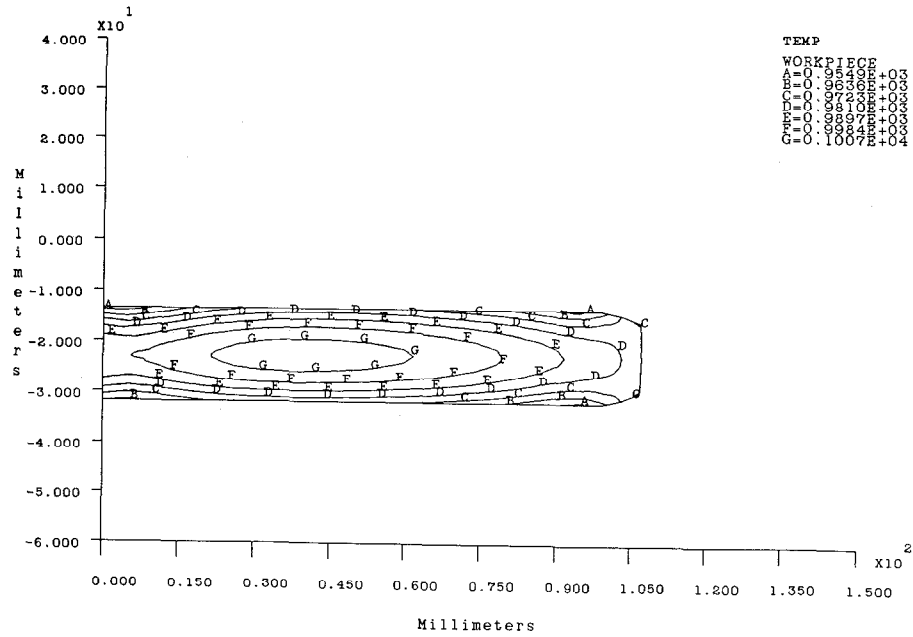


Figure 10. Predicted Temperature Distribution in Forging No. 3

FORGING NO 3 (Isothermal)

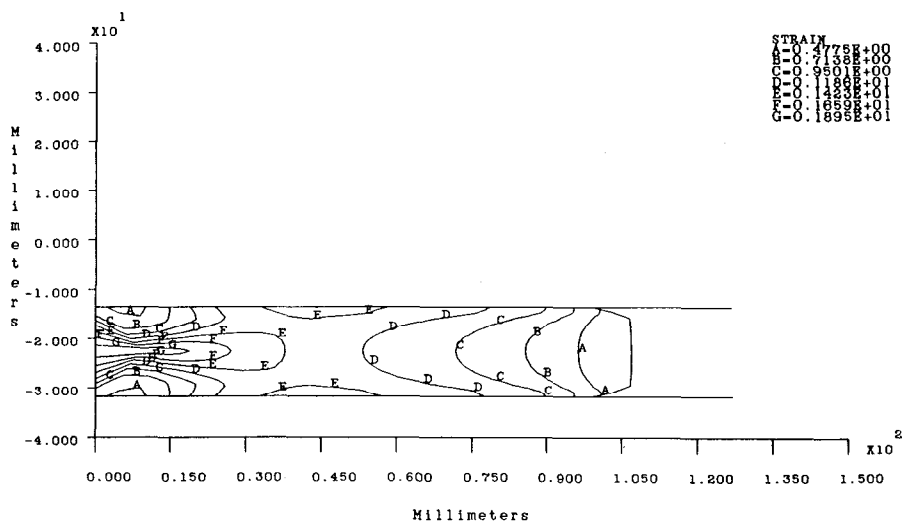


Figure 11. Strain Distribution in an Isothermal Forging

Figure 12 shows the predicted strain distribution in Forging No. 9. Hardness was measured at several locations on the cross section of the forged specimen. Figure 13 shows the variation of hardness with position along lines AA and BB, which are in the hub and in the initially tapered section, respectively. Along line AA, the hardness is greatest at the middle, whereas along line BB the hardness is higher at the top and bottom surfaces. This trend is the same as that observed for the strain distributions in Figure 12.

The hub region and the initially tapered section of the workpiece undergo different deformation paths during the forging operation. The deformation of the hub region of the double wedge specimen is similar to uniaxial compression, i.e., it is subject to axial compression from the start of deformation. The initially tapered section of the specimen is, however, first subject to hoop strain during the deformation of the hub, and then axial strain after the surfaces come in contact with the dies. Figure 14 shows the starting microstructure of the forging stock. Figure 15 shows the microstructure at different locations in Forging No. 9. The regions with high predicted strains have a smaller grain size than regions with low predicted strains, both in the hub and in the initially tapered region of the disk. Close to the axis of symmetry (line AA), regions near the top and bottom surfaces have undergone a small amount of deformation ($\epsilon \cong .8$), and the microstructure shows deformed grains. The center of the disk has, however, been subject to high strain ($\epsilon > 2.0$), and has recrystallized to a fine grain size. In the initially tapered section of the disk (line BB), the regions close to the top and bottom surfaces have undergone greater deformation ($\epsilon \cong 1.5$) than the region in the middle ($\epsilon \cong 1.2$). The regions close to the surface have recrystallized to a fine grain size, while the middle is partially recrystallized, showing a mixed grain size structure. Differences in the microstructure between the top and bottom surfaces is probably due to differing frictional effects. The hardness variations are due to the different grain sizes in the various locations.

Summary and Conclusions

1. Empirical constitutive equations to describe the flow behavior of fine grain IN-718 were developed from isothermal constant true strain rate compression tests.
2. The non-isothermal forging of a double wedge billet to a disk was simulated by incorporating the constitutive equations, along with relevant thermal and interface property data, into the rigid-viscoplastic finite element code ALPID.
3. The load-stroke curves obtained from the simulations showed good agreement with data from physical forgings.
4. The trends in the predicted strain distributions followed trends in the measured hardness and grain size in the forged specimens.
5. This study shows that if material properties under forging conditions are available, process models that accurately describe the characteristics of the forging process can be developed.

References

1. ASM Metals Reference Book, Second Edition, (Metals Park, OH: American Society for Metals, 1983).
2. J. H. Holloman, "Tensile Deformation," *Trans. AIME*, 162, (1945), 258-290.

3. H. W. Swift, "Plastic Instability under Plane Stress," *J, Mech. Phys. Sol.*, 1, (1952), 1-8.
4. W. H. Hosford and R. M. Caddell, Metal Forming: Mechanics and Metallurgy, (Prentiss-Hall, Inc. Englewood Cliffs, NJ, 1983) 115.
5. W. T. Wu and S. I. Oh, "ALPID-T: A General Purpose FEM Code for Simulation of Nonisothermal Forming Processes," 13th NAMRC, North American Manufacturing Research Conference Proceedings, (North American Manufacturing Institution of SME, Dearborn, MI, 1985), 449-455.
6. J. F. Thomas, Jr. and R. Srinivasan, "Constitutive Equations for High Temperature Deformation," *Computer Simulation in Materials Science*, ed. R. J. Arsenault, J. R. Beeler, Jr., and D. M. Easterling, (ASM International, Materials Park, OH, 1988), 269-290.
7. P. C. Charpentier, et al., "Characterization and Modeling of the High Temperature Flow Behavior of Aluminum Alloy 2024," *Metallurgical Transactions A*, 17A, 1986, 2227-2237.
8. A. T. Male and M. G. Cockcroft, "A Method for the Determination of the Coefficient of Friction of METals Under Conditions of Bulk Plastic Deformation," *Journal of the Institute of Metals*, 93, (1964) 38.
9. C. H. Lee and T. Altan, "Influence of Flow Stress and Friction Upon Metal Flow in Upset Forging of Rings and Cylinders," *Journal of Engineering for Industry*, 1972, 775-782.
10. V. K. Jain and R. L. Goetz, "Determination of Contact Heat-Transfer Coefficient for Forging of High-Temperature Materials," (presented at the ASME National Conference on Heat Transfer, Minneapolis, 26-31 July 1991)
11. R. E. Taylor, H. Groot and J. Larimore, "Thermophysical Properties of IN-718 and H-13 Alloys: A Report to Wright State University," (Report TPRL 854, Purdue University, 1989).

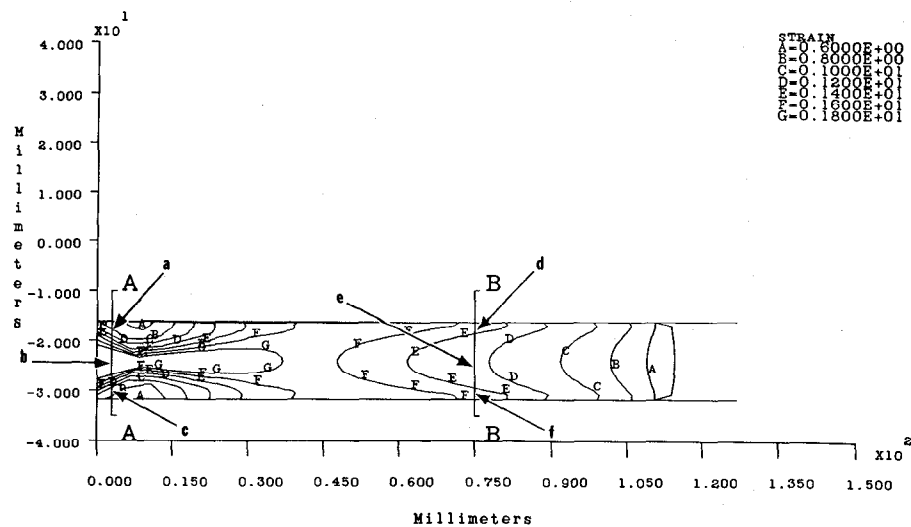


Figure 12. Strain Distribution in Forging No. 9

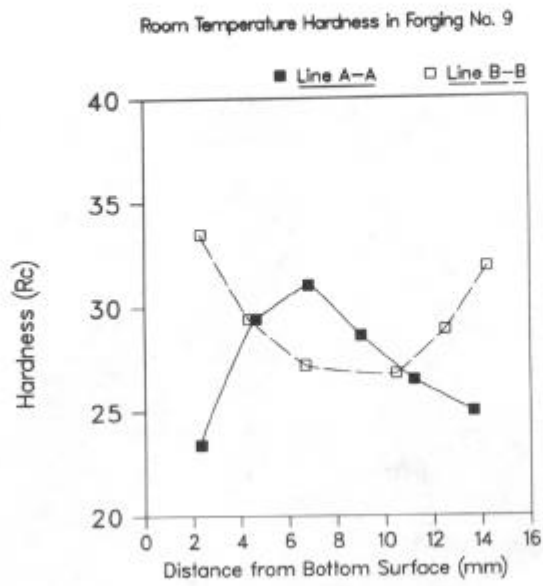


Figure 13. Hardness Variations along lines AA and BB in Figure 12

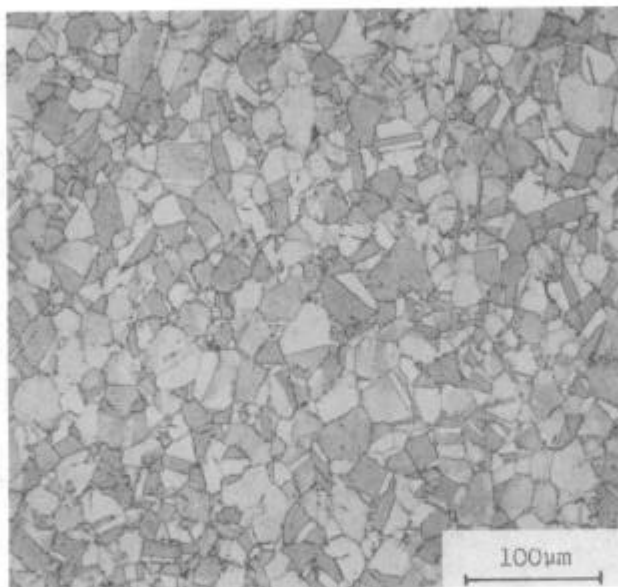
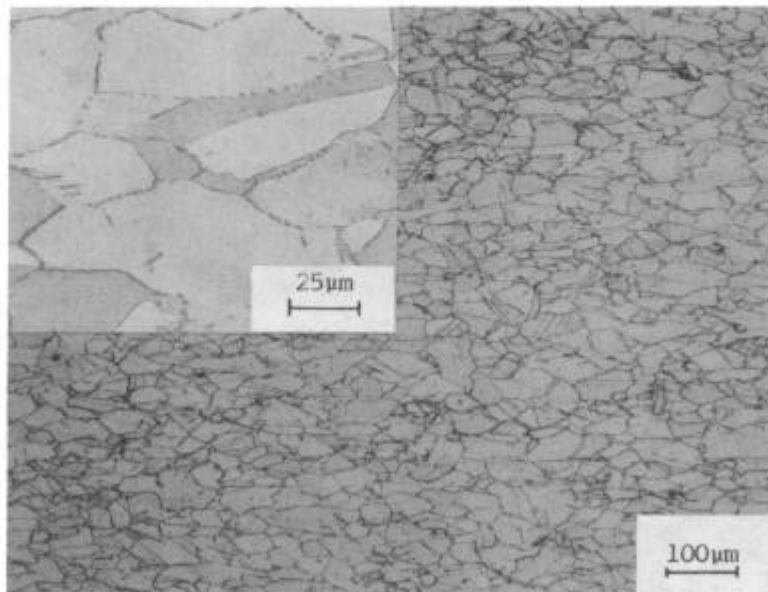
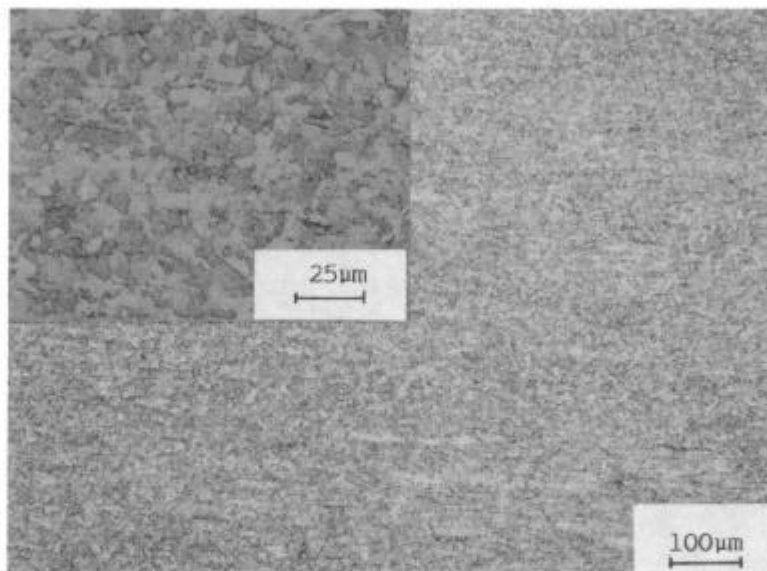


Figure 14 The Starting Microstructure

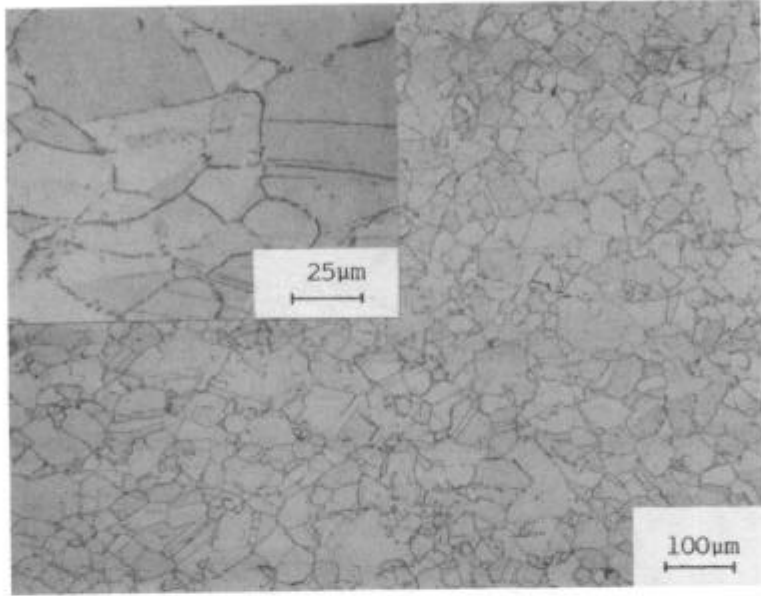


(a)

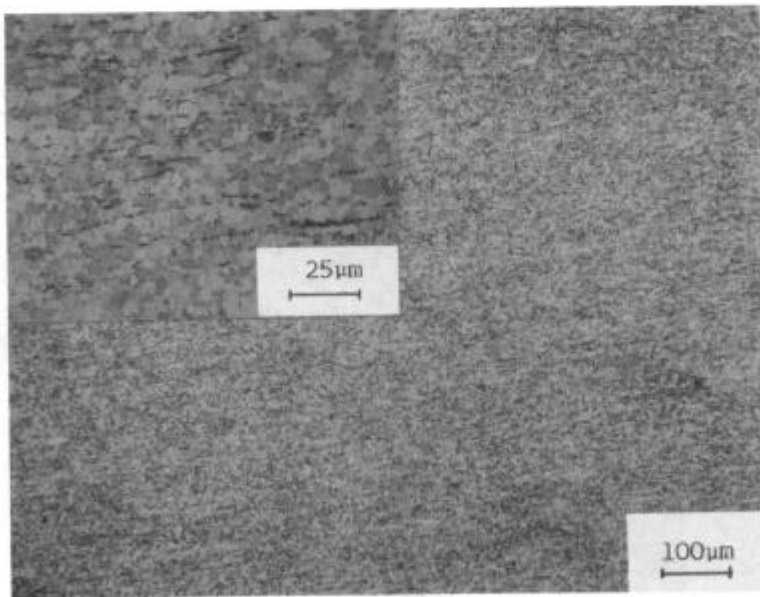


(b)

Figure 15 Microstructures at locations (a), (b), (c), (d), (e) and (f) in Figure 12

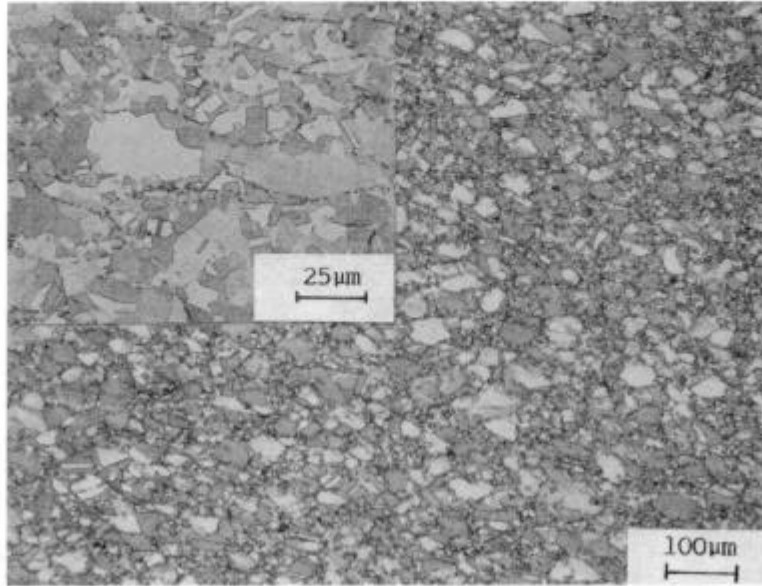


(c)

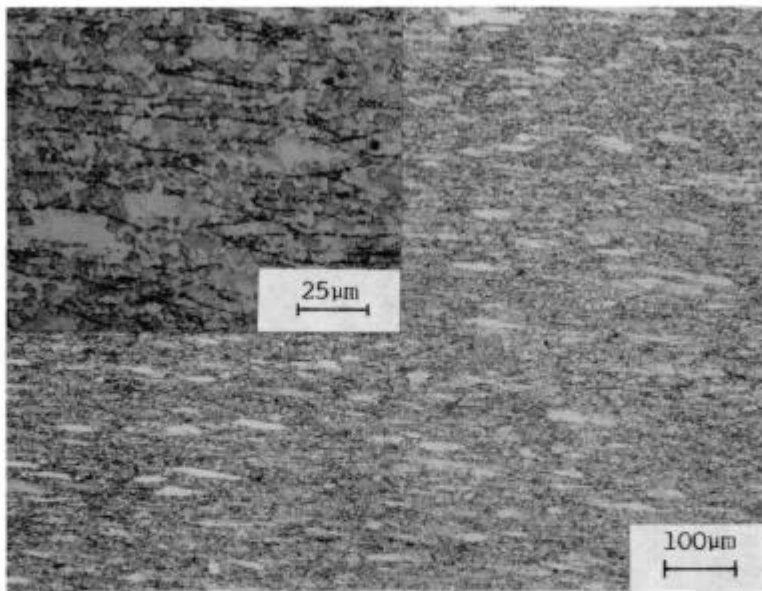


(d)

Figure 15 (cont.)



(e)



(f)

Figure 15 (cont)